Sequential Grafting of Dielectric Phosphates onto Silicon Oxide

G. Freiman,[†,‡] P. Barboux,*,[§] J. Perrière,[∥] and K. Giannakopoulos[⊥]

*Laboratoire de Physique de la Matière Condensée, CNRS UMR 7643, Ecole Polytechnique,
91128 Palaiseau Cedex, France; STMicroelectronics, 850 rue Jean Monnet, 38926 Crolles Cedex, France;
Laboratoire de Chimie de la Matière Condensée, CNRS UMR 7574, ENSCP,
11 rue P. et M. Curie, 75005 Paris; Institut des NanoSciences de Paris,
CNRS UMR 7588-Université Paris 6, Campus Boucicaut,
140 rue de Lourmel, 75015 Paris; and Institute of Material Science, NCSR Demokritos, Athens, Greece*

This work explores the growth of high-*k* oxide films deposited onto silicon by original synthesis methods based on wet chemistry, either aqueous or organic. Zirconium and titanium phosphate layers have been deposited by alternate dipping sequences in diluted solutions of monomeric Ti or Zr alkoxides (M) and phosphoric acid (P). The films have been characterized by dynamic contact angle measurements with water, infrared spectroscopy, X-ray reflectometry, HRTEM microscopy, and Rutherford backscattering spectroscopy. The composition of the zirconium phosphate films corresponds to a P/Zr = 1 ratio, induced by the dipping sequence, and not to that defined by thermodynamic conditions that would precipitate a P/Zr = 2 composition. The growth rate shows that, in optimized conditions, dense monolayers can be deposited during each cycle. The dielectric properties indicate a high dielectric constant that decreases upon dehydration at 300 °C. The static dielectric constant measured at 1 kHz in capacitance–voltage geometry is around 40 for the films heat-treated at 300 °C in air.

1. Introduction

The continuously downscaling of the metal–oxide–semiconductor (MOS) systems needs the integration of new components, particularly new gate oxides that should have a dielectric constant higher than SiO_2 (ϵ = 3.8) and a large band gap to avoid leakage currents.[1–3] At the same time, nanotechnology tends to develop new systems on silicon for molecular electronics or biological functions. Therefore, there is a request for grafting onto silicon new materials which may be hybrid systems, both organic and mineral, that could not be deposited with the usual vacuum evaporation techniques (chemical vapor deposition, atomic layer vapor deposition, etc.). Moreover, phosphates and phosphonates offer a good alternative to silanes as a coupling agent between mineral and organic layers. Phosphate layers can thus be used as a good buffer layer and could allow grafting biological or organic functions onto the mineral surface of Si or SiO_2. The phosphate bond to zirconium or titanium is particularly stable.[4] For this reason, we developed our approach on the synthesis of metal phosphates layers onto silicon using a layer-by-layer approach.

The layer-by-layer deposition method has been described already 10 years ago for polyelectrolyte systems.[5–8] It allows the fabrication of ultrathin films. For mineral systems, first attempts were made with metal phosphonates. Indeed, zirconium and titanium phosphonates form bidimensional layered compounds that are easily deposited as multilayers onto a silicon wafer.[9,10] These methods could be successfully generalized to complex oxides such as niobates[11] or perovskites.[12] Ionic layer deposition is also a mean to deposit a large variety of oxides, hydroxides, or sulfides.[13] Recently, some reports have also appeared on the deposition of heterostructures based on alternate layer deposition of ionic colloidal species such as phosphates,[14,15] lamellar clays,[16] or oxides.[17] Development of high-*k* metal oxide ultrathin

* To whom correspondence should be addressed. E-mail: philippe-barboux@enscp.fr.

[†] CNRS UMR 7643.
[‡] STMicroelectronics.
[§] CNRS UMR 7574.
[∥] Université Paris 6.
[⊥] NCSR Demokritos.

(1) Buriak, J. M. *Chem. Rev.* **2002,** *102,* 1272.
(2) Houssa, M. *High-K Gate Dielectrics*; Institute of Physics: Woodbury, NY, 2004.
(3) Wilk, G. D.; Wallace, R. M.; Anthony, J. M. *J. Appl. Phys.* **2001,** *89,* 5243.
(4) Connor, P. A.; McQuillan, A. J. *Langmuir* **1999,** *15,* 2916.

(5) Fou, A. F.; Ellis, D.; Ferreira, M.; Rubner, M. F. *Polym. Prepr. (Am. Chem. Soc., Div. Polym. Chem.)* **1994,** *35* (1), 221.
(6) Decher, G. *Science* **1997,** *277,* 1232.
(7) Decher, G.; Lehr, B.; Lowack, K.; Lvov, Y. Y.; Schmitt, J. *Biosens. Bioelectron.* **1994,** *9,* 677.
(8) Lvov, Y.; Haas, H.; Decher, G.; Möhwald, H.; Michailov, A.; Mtchedlishvily, B.; Morgunova, E.; Vainshtain, B. *Langmuir* **1994,** *10,* 4232.
(9) Lee, H.; Kepley, L. J.; Hong, H.-G.; Akhter, S.; Mallouk, T. E. *J. Phys. Chem.* **1988,** *92,* 2597.
(10) Katz, H. E.; Schilling, M. L.; Chidsey, C. E. D.; Putvinski, T. M.; Hutton, R. S. *Chem. Mater.* **1991,** *3,* 699.
(11) Fang, M.; Kim, C. H.; Saupe, G. B.; Kim, H.-N.; Waraksa, C. C.; Miwa, T.; Fujishima, A.; Mallouk, T. E. *Chem. Mater.* **1999,** *11,* 1526.
(12) Schaak, R. E.; Mallouk, T. E. *Chem. Mater.* **2000,** *12,* 2513.
(13) Tolstoi, V. P. *Russ. Chem. Rev.* **1993,** *62,* 237.
(14) Keller, S. W.; Kim, H.-N.; Mallouk, T. E. *J. Am. Chem. Soc.* **1994,** *116,* 8817.
(15) Putvinski, T. M.; Schilling, M. L.; Katz, H. E.; Chidsey, C. E. D.; Mujsce, A. M.; Emerson, A. B. *Langmuir* **1990,** *6,* 1567.
(16) Kleinfeld, E. R.; Ferguson, G. S. *Science* **1994,** *265,* 370.
(17) Kovtyukhova, N.; Ollivier, P. J.; Chiznik, S.; Dubravin, A.; Buzanev, E.; Gorchinskiy, A.; Marchenko, A.; Smirnova, N. *Thin Solid Films* **1999,** *337,* 166.
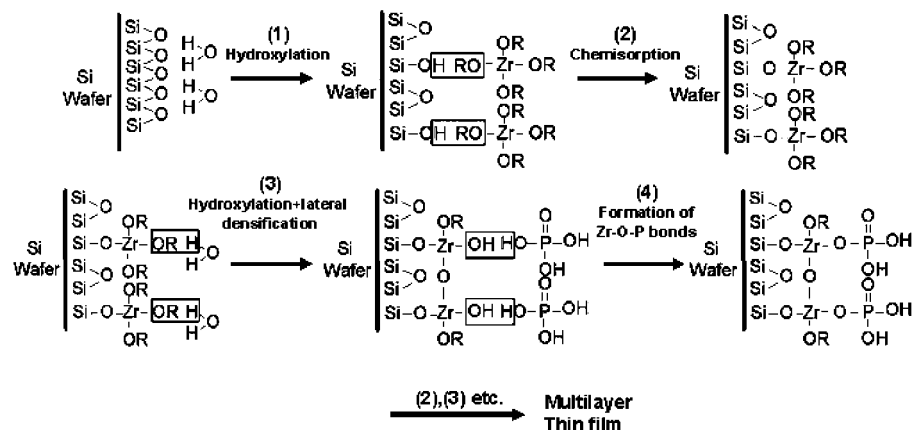
Figure 1. Principle of a sequential deposition of a zirconium phosphate.

films using this method has already been carried out using a similar approach for composite oxides (TiO2–ZrO2–La2O3) by Ichinose et al.[18,19] They emphasized the interest of developing new "surface sol–gel" methods by sequential chemisorption and activation steps that could allow a better control of the film deposition at the molecular level. Indeed, such methods give rise to ultrathin oxide films with higher density than conventional sol–gel deposition that, through the three-dimensional polycondensation of an oxide network, usually yields porous layers. Therefore, this method can be applied to the synthesis of high-*k* dielectric materials with lower porosity.[20] In this work we apply the method to the synthesis of dielectric phosphate films by sequential dipping into solutions of metal alkoxides (Zr or Ti) and phosphoric acid. We discuss the nature of the resulting films and the conditions to obtain single layers for each deposition step.

2. Experimental Section

All reagents were purchased from Aldrich Chemicals. Titanium(IV) isopropoxide and zirconium(IV) *n*-propoxide were used as is. Their corresponding parent alcohols were distilled before use. Phosphoric acid was diluted in bidistilled water. All the experiments except those involving infrared measurements were performed on an n-type Si(100) substrate with a resistivity of 1–10 Ω·cm (ACM supplier) polished on both sides. This yields a conducting substrate that allows dielectric measurements. However, IR spectroscopic investigations were made on a similar undoped Si with two polished faces to avoid absorption by charge carriers. Before the film deposition sequence, the wafer was first treated for 20 min at 80 °C in a piranha solution (mixture of concentrated H2O2 and H2SO4, 25%–75% mixed slowly with caution) in order to remove the organics. Then, the oxide layer was removed by treatment with a 2% HF solution at room temperature for 3–4 min. Then, the silicon wafer was again treated with a fresh piranha solution to reconstruct a well-reproducible oxide layer. This procedure was preferred to thermal oxidation because it yields a hydrated oxide layer (OH-terminated) more suitable for grafting than a siloxane-terminated layer (Si–O–Si).

X-ray reflectometry measurements were carried out on a Philips X'Pert (Cu Kα) equipped with a grazing incidence and reflectometry setup. Data analysis was performed with the Paratt approach[21] using the software Parratt32.[22] The refractive index and thickness were obtained with a VUV Jobin-Yvon ellipsometer. Electron microscopy was performed on a Philips CM20 (200 kV) electron microscope, equipped with energy dispersive X-ray spectrometry (EDS) and electron energy loss spectroscopy (EELS) systems. The composition and thickness of the films were routinely determined by Rutherford backscattering spectrometry (RBS). The precise depth distributions of the various cationic constituents were obtained by the use of the RUMP simulation program.[23] The dielectric properties were obtained in a metal–insulator–semiconductor geometry. The metal consists of an evaporated gold electrode; the insulator consists of the film and the silicon oxide layer. The Si wafer forms the semiconductor with an ohmic back electrode contact formed by a liquid Ga–In alloy painted onto it. The given voltage refers to the voltage difference between the gold top electrode and the silicon back electrode taken as the reference (i.e., $V = V_{Au} − V_{Ga–In}$).

The principle of growth of the phosphate films is described in Figure 1. It is based on the stepwise adsorption of metal alkoxides and phosphoric acid. The wafer is dipped in a dilute solution of alkoxide precursors (titanium isopropoxide in distilled 2-propanol or zirconium *n*-propoxide in *n*-propanol, concentrations studied: 10^{-4}–10^{-2} M). After rinsing with dry absolute ethanol, the solution is dipped into distilled water and then into the dilute solution of phosphoric acid (same concentration as the titanium alkoxide). Again distilled water is used to rinse the phosphoric acid solution. To summarize, one deposition cycle contains the following dipping sequences: alkoxide–absolute ethanol–water–H3PO4–water–absolute ethanol.

The withdrawal rate is chosen such that a limited thickness of liquid is pulled from the solution (with 2 cm/min). Taking into account the physical parameters of the solvent (density, viscosity, and surface tension), we can calculate by means of the Landau–Levich law[24] that less than a few microns of liquid is withdrawn with the substrate.[25] With a precursor concentration between 10^{-4} and 10^{-3} M, less than a tenth of a monolayer can then be deposited by viscous drag of the solution. Although we cannot exclude this phenomenon, we expect that most of the film will be deposited by a grafting reaction of one monolayer per step such as shown in Figure 1. The grafting mechanism that we proposed is based on the chemistry of phosphoric acid reactions with zirconium oxide

(18) Ichinose, I.; Senzu, H.; Kunitake, T. *Chem. Mater.* **1997**, *9*, 1296.
(19) Ichinose, I.; Senzu, H.; Kunitake, T. *Chem. Lett.* **1996**, 831.
(20) Aoki, Y.; Kunitake, T.; Nakao, A. *Chem. Mater.* **2005**, *17*, 450.
(21) Paratt, L. G. *Phys. Rev.* **1954**, *95*, 359.

(22) Braun, C. Parratt32 software, Berlin Neutron Scattering Center, BENSC, Hahn-Meitner Institut, Berlin.
(23) Doolittle, L. R. *Nucl. Instrum. Methods* **1985**, *B9*, 344.
(24) Landau, L. D.; Levich, B. V. *Acta Physicochim. USSR* **1942**, *17*, 42.
(25) de Gennes, P. G.; Brochard-Wyart, F.; Quéré, D. *Capillarity and Wetting Phenomena: Drops, Bubbles, Pearls, Waves*; Springer: New York, 2004.
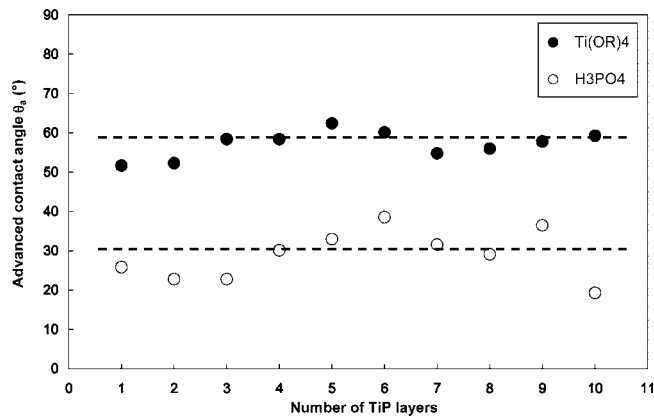
Figure 2. Change of the contact angle (advancing) with pure water as a function of the nature and number of dipping sequences H_3PO_4 and $Ti(OR)_4$ onto silicon.

surface groups[4,26] as well as on previous works that demonstrate the feasibility of sequential adsorption of zirconium salts with phosphonates.[9,27,28] The dipping equipment was fully automated and placed in a glovebox with circulating dry nitrogen and a large layer of silica gel. Since some solutions (phosphoric acid, rinsing water) in the system contain water, this limits the relative humidity to around 25% above the diluted alkoxide solutions as measured by the hygrometer. Since some dipping sequences last for a few hours, the vessels were adapted to maintain a constant level due to alcohol evaporation.

In some experiments applied to the synthesis of a Ti–P film, a balance was placed under the water activation solution (after the Ti step) and rinsing solution (after the phosphoric acid step). This allowed recording the force acting on the liquid, i.e., in the opposite direction, the capillary force acting on the substrate and film. The dynamic contact angle could be extracted from this measurement,[29] as discussed in the Supporting Information. As a function of the rinsing step, we observe a periodical change of value between the Ti-terminated film ($\theta_a = 55°$, measured in the absence of UV light to avoid any potential photocatalytic effect by TiO_2) and the phosphate layer ($\theta_a = 30°$) after the deposition step of phosphoric acid (Figure 2). This indicates the periodical change of contact angle and further exemplifies the alternate change of surface termination.

The film thickness has been analyzed with X-ray reflectometry and VUV ellipsometry. Both techniques agree to yield similar results for the film thickness and the discussion on the refractive index obtained from VUV ellipsometry will be in complete agreement with that on the electron density observed by X-ray reflectometry. So, only X-ray reflectometry will be discussed in the following. The thickness increase for the zirconium phosphate films obtained with *n*-propoxide depends on the concentration (Figure 3b). This indicates that probably more than one monolayer is deposited during each cycle for concentrations above 10^{-3} M. At low concentration of zirconium alkoxide (5×10^{-4} M) a growth rate of 0.7–0.8 nm per cycle is reached corresponding to a monolayer. However, the electron density does not depend on the monomer concentration (Figure 3c) which shows that the films are dense. Also, similar results are obtained for zirconium *n*-propoxide and zirconium *n*-butoxide which have the same reactivity (Figure

(26) Carrière, D.; Moreau, M.; Barboux, P.; Boilot, J. P.; Spalla, O. *Langmuir* **2004**, *20*, 3449.
(27) Katz, H. E.; Schilling, M. L.; Chidsey, C. E. D.; Putvinski, T. M.; Hutton, R. S. *Chem. Mater.* **1991**, *3*, 699.
(28) Gawalt, E. S.; Avaltroni, M. J.; Koch, N.; Schwartz, J. *Langmuir* **2001**, *17*, 5736.
(29) Hayes, R. A.; Robinson, R. C.; Ralston, J. *Langmuir* **1994**, *10*, 2850.
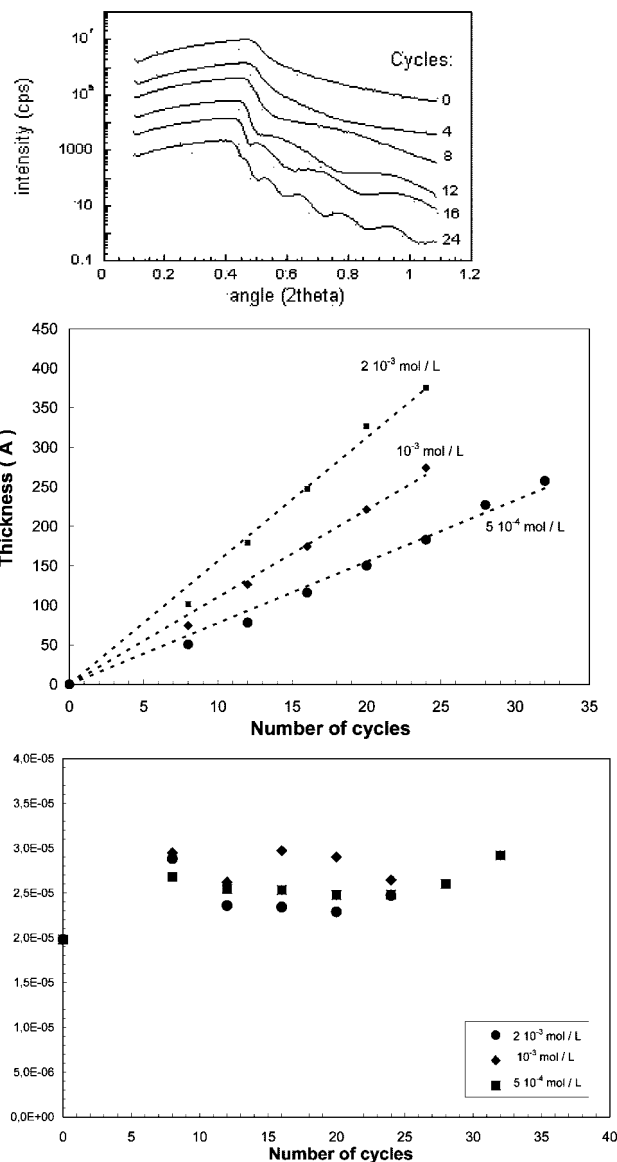
Figure 3. X-ray reflectivity of Zr–(PO_4) layers obtained with different concentrations of zirconium *n*-propoxide as a function of the number of deposition sequences: (a) curves obtained for various deposition cycles; (b) thickness as a function of the number of dipping cycles; (c) electron density obtained by the fits.

4). However, in the case of titanium phosphate, a large difference is observed between titanium isopropoxide and titanium butoxide (Figure 5). The film thickness increases more rapidly in the case of the isopropoxide whereas its density decreases. This is probably associated to the high reactivity of the isopropoxide that reacts very rapidly with the surface and yields a random grafting with a porous layer instead of a dense one. Moreover, it is difficult to completely eliminate the moisture in the process; the isopropoxide may polycondense in the solution, and titanium layers may be grafted as colloidal or oligomeric species. Therefore, denser layer can only be achieved with weakly reactive species such as butoxides.

For the Zr–PO_4 layers, infrared absorption spectroscopy shows the characteristic vibrations of phosphate groups around 1100 cm^{-1} and that of the OH stretching of phosphate (P–OH) or water

Grafting of Dielectric Phosphates onto SiO₂

Chem. Mater., Vol. 19, No. 24, 2007 5865

Figure 4. Thickness and electron density of a Zr–P film obtained with zirconium *n*-propoxide or zirconium butoxide precursors as a function of the number of deposition cycles.
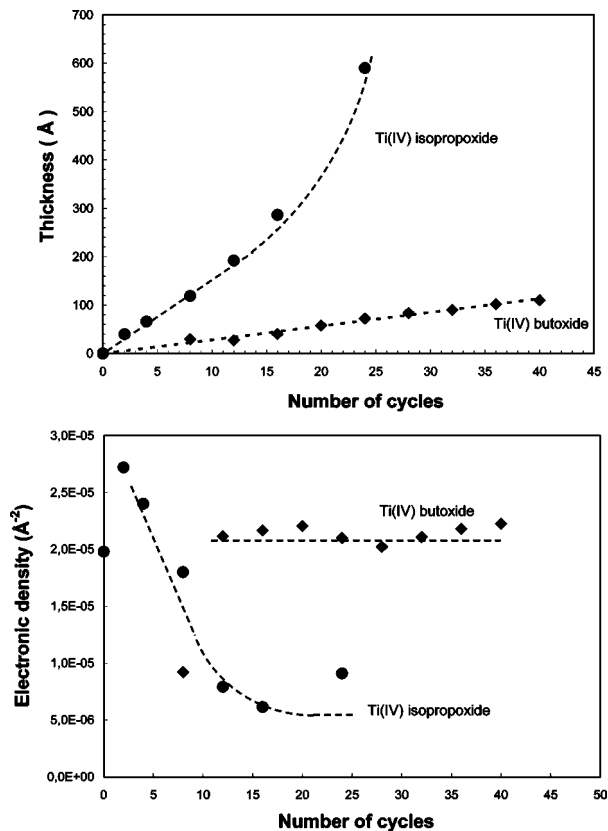
Figure 5. Thickness and electron density of a Ti–P film obtained with titanium *n*-propoxide or titanium butoxide precursors as a function of the number of deposition cycles.
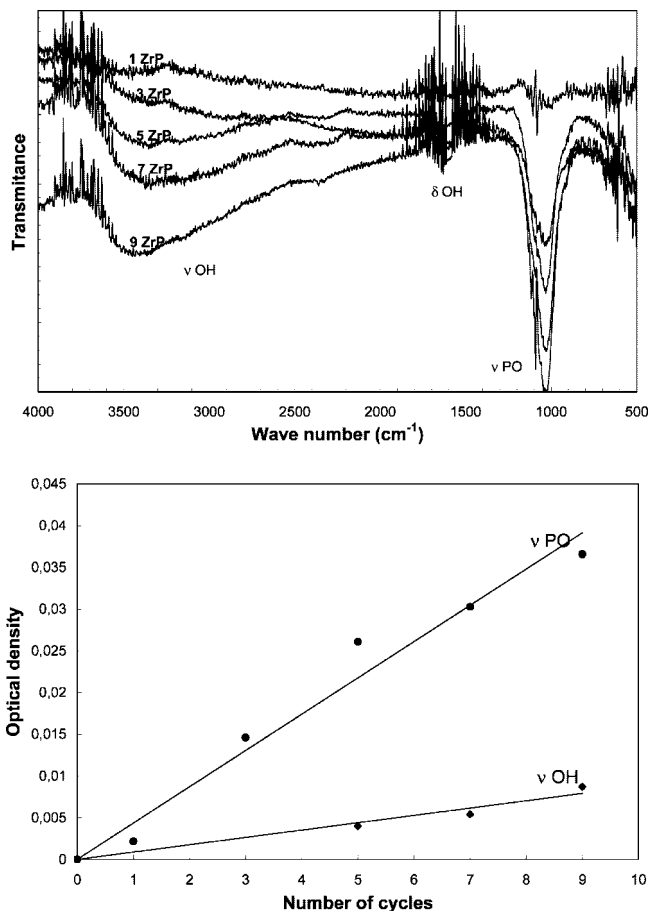
Figure 6. Infrared spectroscopy of a Zr–P film after 1, 2, 4, 7, and 10 cycles. Peak intensity is taken as the maximum height of the OH and PO vibrations as a function of the number of deposition cycles.
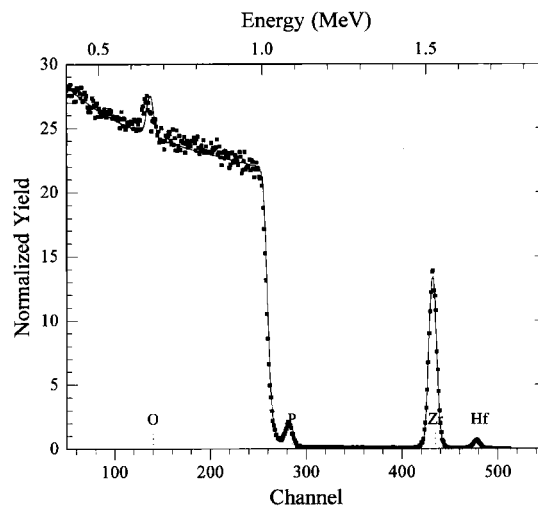
Figure 7. RBS of a ZrO₂–H₃PO₄ film (24 cycles) and simulation with the nominal composition ZrHPO$_{5.1}$. Hafnium is present as an impurity in zirconium (2%). Simulation using the RUMP program.[23]

molecules at approximately 3500 and 1610 cm^{-1}. The films contain thus water and grow as a hydrated phosphate. Both vibrations increase linearly with the number of cycles (Figure 6).

The films composition has been analyzed by Rutherford back-scattering spectrometry (Figure 7). Simulations have been based on a three-layer model: Si(infinite layer)/SiO₂(30 ×10^{15} atoms/cm²)/film. For the films deposited at a concentration above 1 × 10^{-3} M, a good simulation of the spectra is obtained with the

Table 1. Data for Films of Zr–PO$_4$ (Zirconium *n*-Propoxide) Showing the Composition and Total Atom Density of the Layer As Determined from RBS^a

no. of cycles, concentration	composition (first layer)	density ($\times 10^{15}$ atoms/cm^2)	e_{RBS} (nm)	$e_{reflecto}$ (nm)	$e_{ellipso}$ (nm)
24, 2 × 10^{-3} M	ZrP$_{0.95}$O$_{5.1}$	175	35	43	39
24, 2 × 10^{-3} M	ZrP$_1$O$_{5.1}$	130	26	37	33
24, 1 × 10^{-3} M	ZrP$_{0.9}$O$_{5.2}$Si$_{0.1}$	140	28	27	30
32, 5 × 10^{-4} M	ZrP$_1$O$_{5.5}$Si$_{0.25}$	120	24	25	28

^{a} The thickness estimated by RBS from the composition and atomic density of atoms is compared to those measured by X-ray reflectometry and ellipsometry.
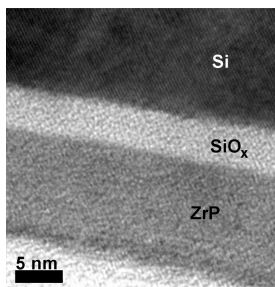
Figure 8. Transmission electron microscopy cross-sectional image of a zirconium phosphate layer deposited after 25 cycles and annealed at 300 °C for 30 min in air (concentration of the solution: 2 × 10^{-3} M).

composition O/P/Zr = 5/1/1, in very good agreement with that expected from the alternate deposition sequence of zirconium and phosphoric acid: this nominal composition can be understood as an equal mixture of ZrO$_2$–Zr(HPO$_4$)$_2$, the two stable phases identified in the phase diagram, but it seems that during each cycle the films do not reorganize to form the stable phosphate Zr(HPO$_4$)$_2$, which would give the composition O/P/Zr = 8/2/1.

Since we ignore the chemical nature of the film, it is difficult to estimate their porosity. This can still be estimated by the comparison between the RBS results on one side and the reflectometry on the other side. Indeed, RBS results are obtained from the fits and yield the total number of atoms per cm^2 in a phosphate layer. The fits to the curves allow distributing these atoms among Z, P, and O. A general law states that, in most oxides, the oxygen packing forms the volume of the network with all cations occupying the interstices. In all common oxides, the oxygen surface density is 1.5 × 10^{15} atoms/cm^2 (±10%) for a thickness of 0.26 nm (±10%) per oxygen layer. With this assumption, we can estimate a thickness from the RBS, which would be the thickness of a dense oxide or phosphate. The results are given in Table 1 and compared with those of reflectometry and ellipsometry. There is a good agreement between all techniques indicating a low porosity. This probably indicates some porosity, but the difference can be also attributed to the presence of hydration water that disappears under vacuum (in the RBS experiment). In air, the film composition could be ZrO$_2$–H$_2$O–(HPO$_4$–Zr–PO$_4$H)–H$_2$O. Also, for the films deposited with the lower concentrations, silicon must be included in the simulation of the first oxide layer, which may indicate pinholes or an imperfect coverage of the film.

Transmission electron microscopy has been performed on a film deposited by 25 cycles of zirconium *n*-propoxide (2 × 10^{-3} M) and heat-treated at 300 °C for 30 min under oxygen (Figure 8 shows a cross-sectional view). The film is amorphous and highly homogeneous. The thickness of the ZrP and SiO$_2$ layers can be estimated to be 12 and 3.7 nm, respectively, in good agreement with both reflectometry and ellipsometry.

The dielectric constant of the zirconium phosphate films has been estimated through MIS junction measurements on n-type silicon with Ga/In ohmic contacts at the backside. A typical *C*–*V* behavior
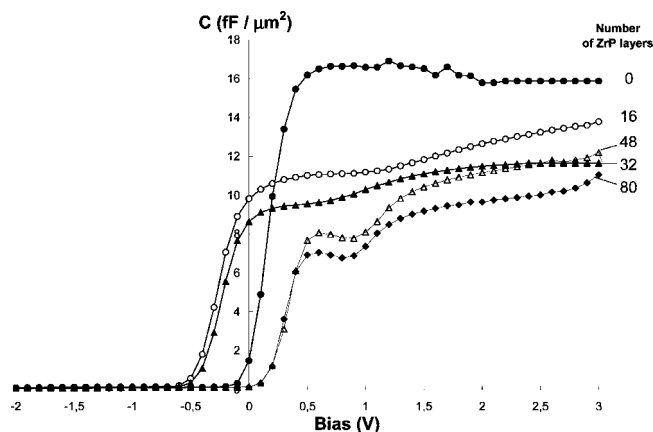
Figure 9. Dielectric capacitance (in nF) as a function of the applied voltage (V) for zirconium phosphate layers deposited with *n*-propoxide (concentration of the solution: 2 × 10^{-3} M); electrode area $S = 4 \times 10^{-2}$ cm^2, $F = 1$ kHz.

is observed (Figure 9), which is characteristic of a semiconductor–insulating oxide–metal junction (MIS type). When the potential of the gold electrode is turned positive, the negative charge carriers of the n-type silicon accumulate to the electrode and a sudden jump of the capacity is observed. For rather similar samples, large changes are observed in the flat band potential (roughly, the potential when the sudden increase occurs) that we cannot explain for the moment (different space charge effect at the semiconductor–phosphate interface due to different hydration levels, pinholes). The surface capacity (nF/cm^2) has been estimated as the high voltages limit, i.e., the value on the plateau at 2 V. Its value is low since it corresponds to the dielectric contribution of two capacitors in series (the SiO$_2$ layer and the phosphate film). The total capacity C_{tot} is therefore given by the formula

$$\frac{1}{C_{tot}} = \frac{1}{C_{SiO_2}} + \frac{1}{C_{phos}} = \frac{1}{C_{SiO_2}} + \frac{ne}{\epsilon_{phos}\epsilon_0} \qquad (1)$$

where C_{SiO_2} and C_{phos} are the capacity of the SiO$_2$ and metal phosphate layer, respectively. The total film thickness is *ne* as obtained after *n* cycles depositing an elementary thickness *e* and having a relative dielectric constant ϵ_{phos}. From the capacity of the film without phosphate film and using a dielectric constant of 3.8 for SiO$_2$, a reasonable thickness of 3–4 nm can be estimated for the SiO$_2$ layer. This is in good agreement with the SiO$_2$ thickness measurements using all techniques. The dielectric capacity of the film as grown and after heat treatment at 300 °C in air is reported in Figure 10. For the phosphate films as deposited, the total capacitance barely depends on the number of deposition cycles or the film thickness. Using an estimate of the film thickness given by X-ray reflectometry and the difference of capacity between the films and the substrate without film yields an estimation of a high dielectric constant $\epsilon_{phos} = 300$. But, this should not be surprising since it probably corresponds to a hydrated compound. After heat treatment at 300 °C for 30 min in oxygen, the capacity depends on the number of cycles (Figure 10). The static dielectric constant can be estimated by the fit of formula 1 to the capacity. The dielectric constant measured at 1 kHz in capacitance–voltage geometry is around 40 for the films heat-treated at 300 °C. Thus, because of the presence of hydrogen bonds or hydration, these materials possess a high dielectric constant but with a limited technological interest due to their weak stability regarding dehydration. Further studies on thermal SiO$_2$ sublayers will try to evaluate the behavior of the anhydrous systems.

Grafting of Dielectric Phosphates onto SiO₂

Chem. Mater., Vol. 19, No. 24, 2007 **5867**
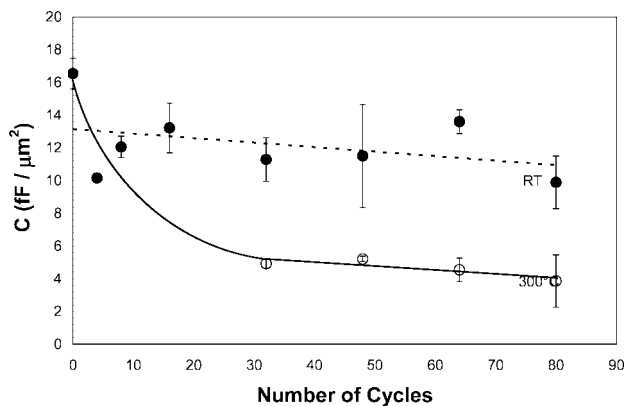
Figure 10. Dielectric capacity of zirconium phosphate layers deposited with with *n*-propoxide (2×10^{-3} M) as a function of the number of deposition cycles (electrode surface area $S = 4 \times 10^{-2}$ cm²).

3. Conclusion and Perspectives

The stepwise assembly of zirconium and titanium phosphate using wet chemistry approach leads to original materials that cannot be obtained by classical evaporation methods. Because of the sequential geometry of deposition, these materials present a composition M/P = 1 that could not be obtained using conditions leading to thermodynamic stability. After heat treatment at 300 °C, they still present a high dielectric constant ($\epsilon_{phos} = 40$). The concentration of the monomers and their reactivity must be optimized in order to deposit one single dense monolayer at each cycle. The denser films are obtained when the reactivity of the monomer solution is low when compared to that between the monomer solution and the activated surface.

Supporting Information Available: Schematic view of the automated dipping machine; measurements of capillary forces and contact angle of film. This material is available free of charge via the Internet at http://pubs.acs.org.